Full Length Research Paper

Mapping Quaternary deposits in the el-Jufr playa (Southeastern Jordan Plateau) using geoelectrical techniques: Implications for geology and hydrogeology

Awni T. Batayneh

Department of Geology and Geophysics, King Saud University, P. O. Box 2455, Riyadh 11451, Saudi Arabia.

Geoelectrical measurements using the vertical electrical sounding method were conducted on the el-Jufr playa, Southeastern Jordan Plateau. The objectives of the study were (i) to observe, map and describe the range of difference in Quaternary deposits, and (ii) to identify formations that may present fresh aquifer waters, and subsequently to understand the relationship between possible groundwater resources and structural elements. Data collected at 20 locations were interpreted first with curve-matching techniques, using theoretically calculated master curves. The initial earth models were double-checked and reinterpreted using a one-dimensional inversion program in order to obtain the final subsurface electrical stratigraphy units, including the water-bearing aquifer. The results of interpretation are used to construct litho-resistivity cross sections across the study area in light of the surface and subsurface geologic information. The inspection of litho-resistivity cross sections reveals the presence of two main alluvial sequences. The upper sequence that attains resistivities ranging from 5 to 120 ohm-m and thickness ranging from 6 to 18 m are a mixture of reworked aeolian and alluvial sediments. The resistivity of this unit generally decreases south- and central-wards, indicating more homogeneous fine silty sand nature of the Pleistocene sediments. The lower stratigraphic sequence is the shallow sand and gravel layer saturated with fresh water. This layer is characterized by its relatively high resistivity (60 to 400 ohm-m) and varying thickness (8 to 23 m) in the northern and eastern sides and by its relatively low resistivity (20 to 90 ohm-m) and varying thickness (10 to 40 m) in the southern side.

Key words: Jordan Plateau, geoelectric method, geology, groundwater.

INTRODUCTION

Jordan is considered among the poorest countries in the world in terms of water resources. The climate is generally arid to semi arid region where around 90% of the country's land receives an average precipitation of less than 100 mm/year while only 3% of the land receives an average annual precipitation of 400 mm. The pattern of rainfall is characterized by an uneven distribution over the various regions, and strong fluctuation from year to year in terms of quantity and timing (Jordan Meteorological Department, 2010 (personal communication)). While water resources in Jordan are limited, the depletion of non-renewable resources due to over pumping from oppressed aquifers is considered a serious threat to the water sector in Jordan. Moreover, the available re-newable water resources are dropping drastically due to the steep population growth, rapid agricultural and industrial developments and the sudden influx of refugees due to political instability in the region. Several previous studies relating to the water sector in Jordan have generally concluded that there is a need to focus attention on the future impact of water shortages through resources planning and development (Al-Jayyousi and Shatanawi, 1995; Jaber and Mohsen, 2001; Mohsen and

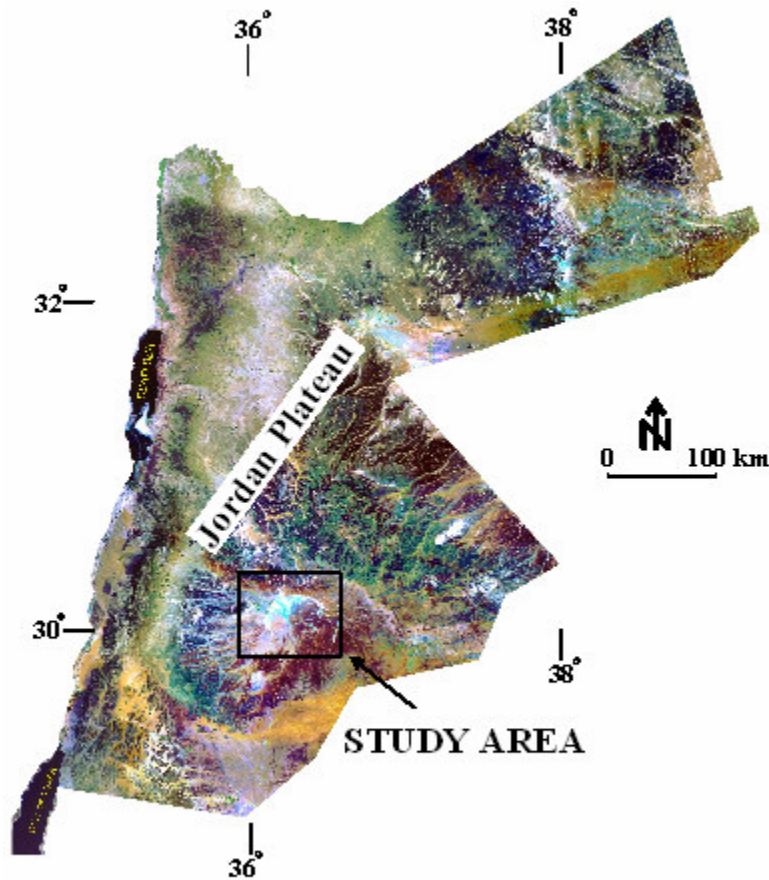*Corresponding author. E-mail: awni@ksu.edu.sa. Tel: +966-56-8086395. Fax: +966-1-4675804.

Figure 1. LandSAT of Jordan Plateau (35°30'-37°30' E by 29°30'-32° 00' N) with location el-Jufr playa.

Jaber, 2002; Jaffe and Al-Jayyousi, 2002; Hadadin and Tarawneh, 2007; Mohsen, 2007; Ta'any et al., 2007; Batayneh et al., 2008).

In the present study, vertical electrical sounding (VES) survey were performed on 20 sites with the aims: (1) observe, map and describe the range of difference in Quaternary deposits available in the el-Jufr playa and (2) identify the formations that may have fresh aquifer waters, and subsequently, understand the relationship between groundwater resources and geological structures.

Location, geology and hydrogeology

The Central Jordan Plateau roughly spreads 35° 30' to 37° 30' E longitude by 29° 30' to 32° 00' N latitude, having elevations ranging from 1,700 m at the western escarpment to 900 to 500 m in playa lakes of the eastern desert. It is dominated by eastern gently sloping topography and numerous playa lakes, that is, characterized by flat topped surface of clays, mud, and salt, obviously seen across LandSat imagery (Figure 1). In total, playas cover an area of 40% of the Jordan eastern desert. The

number and size of these playas and their deposits are, therefore, clearly indicative of moister past environments. The most notable of these playas is the el-Jufr, which is located in the southeast region of the Jordan Plateau (Figure 1).

The 1:100,000 geological map, prepared by the Natural Resources Authority of Jordan (Moumani, 2006) demonstrate that the geology of central Jordan is a part of the Late Cretaceous-Early Tertiary Arabian carbonate platform, which is mainly controlled by the regression of the Tethys Ocean and the tectonic up-warping of the Arabian-Nubian Shield along the Dead Sea Rift (Moh'd, 1986; Powell, 1989). It is covered mainly by shallow marine carbonates that are dissected by a number of regional faults that trend E-W, N-S, NE-SW, and NW-SE. The landscape is controlled by the main valleys that trend towards the north and northeast. The oldest rock formation that outcrops around the el-Jufr playas area is the Muwaqqar Chalk-Marl (MCM) formation (Maastrichtian to Paleocene in age), which is part of the Belqa Group (Moumani, 2006). In the el-Jufr area (Figure 2), only the upper few meters (~20 m) of the formation are exposed. These mainly consist of soft pale yellow, light grey, yellowish to reddish and brown green,
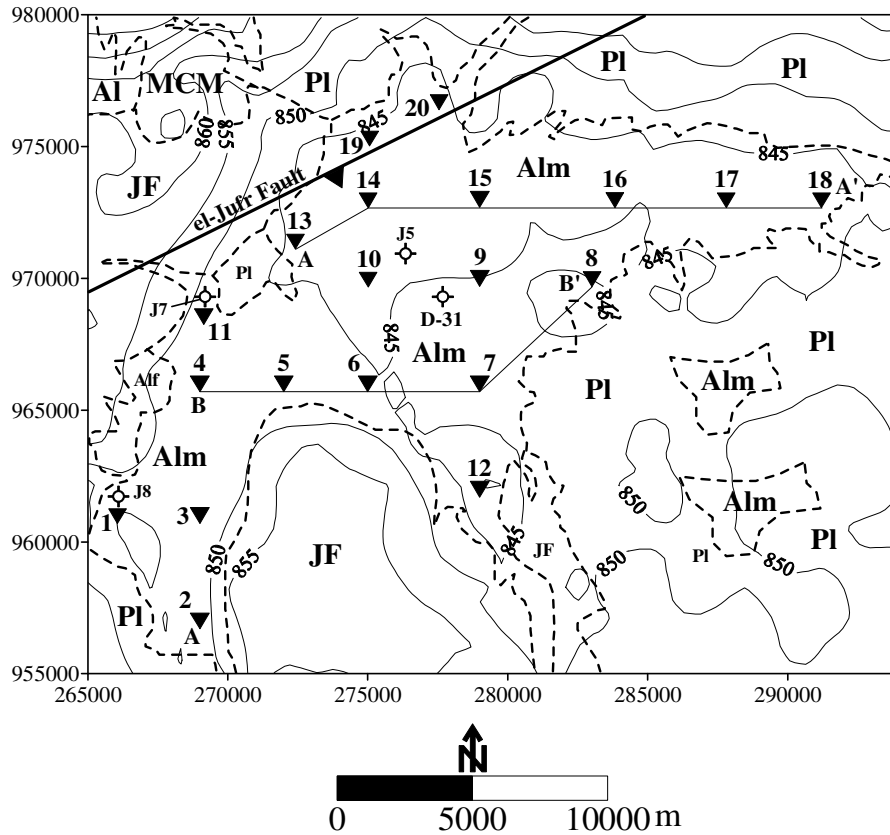
Figure 2. Location of VES sites (black triangle) in relation to geology. Also, shown is the location of two profile lines A-A' and B-B' and four boreholes. The elevation contours are in meters. Palestine grid are used.

occasionally whitish cream chalky marl and marly limestone with gypsum occurs as thin bands or together with calcite in extensional joints. The presence of diverse planktonic fauna, erosional surfaces and ammonites in the MCM formation suggest that these sediments were deposited in a moderate to deep-water pelagic environment (Powell, 1989; Moumani, 2006).

The MCM formation is unconformably overlain by alluvial and lacustrine lake sediments of el-Jufr (JF) formation (Late Pleistocene in age) reaching approximately 5 to 8 m thick. It is mainly composed of conglomerates, marl, sand, clay, and calcrete. Surface deposits within the playas lake consist of unconsolidated terrestrial, aeolian, fluvial, and lacustrine sediments

(Moumani, 2006). Other sediments include fluvial gravels, lacustrine limestones, sandy limestones, marls, and gypsum. The lake is rimmed on the north and northwest by eroding 50 m high limestone and chert plateau, the weathering products of which are carried towards the center of the lake. At the center of the el-Jufr playas, lies an evaporate basin of mudflat and gypsum.

Generally, the groundwater aquifers of Jordan are divided into three main hydraulic complexes (Rimawi et al., 1992), that is, the Deep Sandstone Aquifer Complex, the Upper Cretaceous Aquifer Complex, and the Shallow Aquifer Complex. The Upper Cretaceous and the shallow aquifers is the primary source of water for domestic and industrial uses in the region. The recharge to these
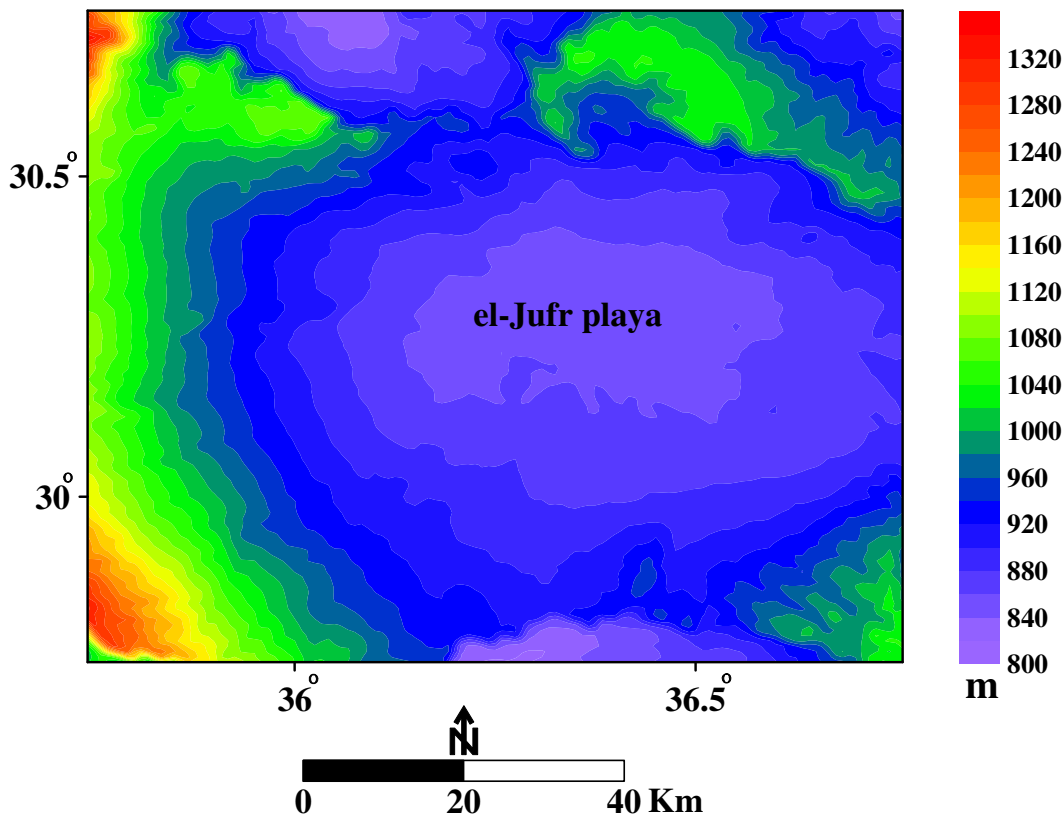
Figure 3. Drainage systems of southeastern Jordan Plateau.

aquifers takes place either from the elevated areas to the east, north and west sides, or due to local surface water infiltrations. The local drainage system is typically characterized by a centripetal pattern with all Wadis draining to the central of the el-Jufr playas from the encircling highlands (Davies, 2005; Moumani, 2006). The drainage patterns in the southeastern Jordan Plateau area are shown in Figure 3. This map is based on topographic data of the terrain elevation model (Geosoft, 2003).

FIELD MEASUREMENTS AND METHODS OF INTERPRETATION

Surface resistivity methods have been applied worldwide to investigate the shallow subsurface of the geological, environmental, geotechnical, and hydrogeological problems. They have proven to be efficient and successful in delineating aquifers and mapped subsurface lithology and geological structures (Batayneh et al., 1999; Batayneh, 2004; Batayneh and Barjous, 2005; Batayneh, 2006). These methods have been widely applied over the last few decades to address the growing need for a non-invasive and cost-effective way to assist in the characterization of near-surface lithology, structures and groundwater aquifers.

In general, the resistivity method involves measuring the electrical resistivity of earth materials by introducing an electrical current into the ground and monitoring the potential field developed by the current. The most commonly used electrode configuration for

geoelectrical soundings, and the one used in this field survey, is the Schlumberger array. Four electrodes (two current A and B and two potential M and N) are placed along a straight line on the land surface. The potential difference ($\triangle V$) and the electrical current (I) are measured for each electrode spacing and the apparent resistivity (ρ_a) is calculated by the equation:

$$\rho_a = K\frac{\Delta V}{I} \qquad (\text{ohm - m})$$

Where:

$$K = \pi\frac{\overline{AM}.\overline{AN}}{\overline{MN}}$$ is the geometrical factor that depends on the electrode arrangement for the Schlumberger array.

A reconnaissance field survey was applied to establish the location of the resistivity stations taking into consideration the availability of boreholes in order to calibrate the resistivity data. The localities that are characterized by the presence of salt crust, dunes, vegetations, and recent aeolian deposits were avoided. In this respect, twenty VES stations were established across the study area using a GPS positioning. The data were collected using the SYSCAL-R2 resistivity meter instrument (IRIS Instrument, France). The layout of the survey stations is superimposed on the geologic map in Figure 2. The half distance between the potential electrodes (MN/2) was increased in steps, starting from 0.5 to 40 m in order to obtain a measurable potential difference. The current electrode half
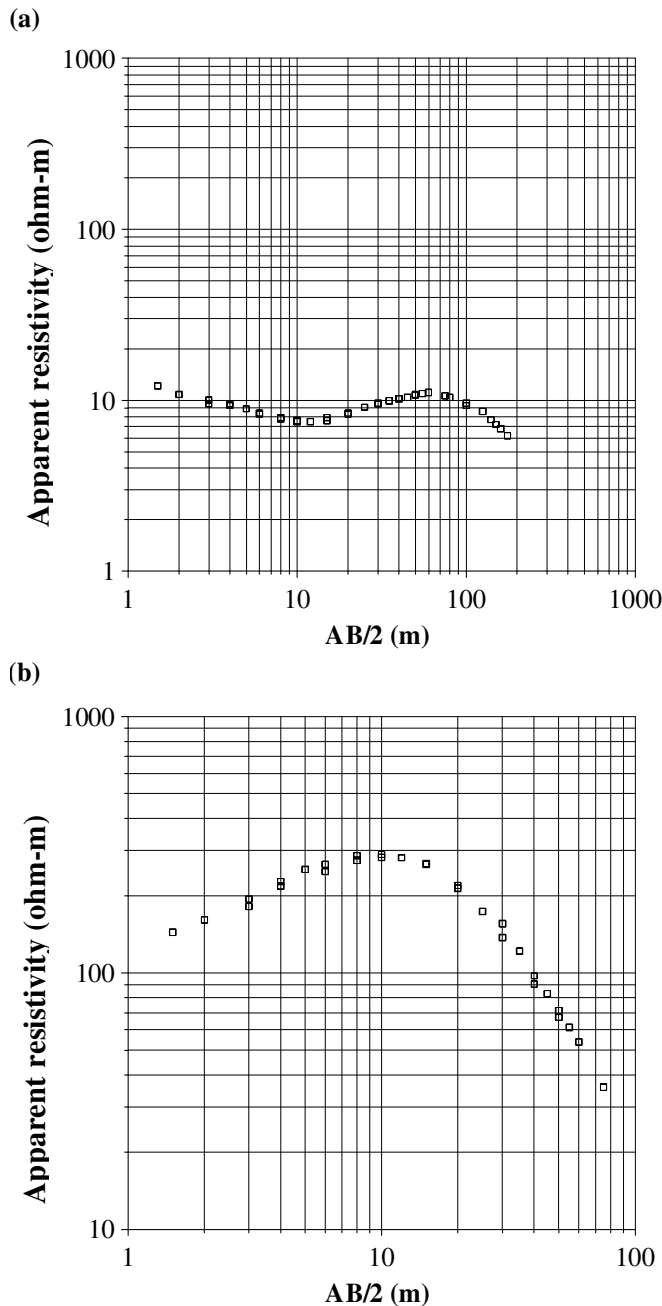
(a)

(b)

Figure 4. Typical field sounding curves.

where the layers resistivity relationship as $\rho_1 < \rho_2 > \rho_3$ (e.g., VES station 18, Figure 4b). Each VES was subjected to two different interpretation techniques: (1) a preliminary interpretation using the partial curve matching technique of Zohdy (1965); Orellana and Mooney (1966). Based on this preliminary interpretation, initial estimates of the resistivities and thickness (layer parameters) of the various geoelectric layers were obtained, and (2) the 1D-inverse modelling using RESIX-IP Software (Interpex Limited, 1999). Summary of the results for all sounding stations are shown in Table 1.

Calibration of VES data

The geoelectric resistivity of sediments is one of the most variable physical properties, especially in a very complicated sedimentological environment that dominates such areas. Earth resistivity is related to important geologic parameters, including types of rocks, types of soils, porosity, degree of saturation, and salinity (Keller and Frischknecht, 1966). However, there are no sharp guidelines to interpret the lithology and/or water content from the contrast in the resistivity layers. Therefore, the ambiguities in interpretation may occur and it is very necessary to calibrate the observed VES data with the available borehole data. This enables us to assign the interpreted geoelectric units to their corresponding lithologic units which consequently put a reliable control on the subsurface sequence interpretation of the study area. For this purpose, data from four boreholes (Figure 2) were analyzed and used to correlate the results of the VES geoelectrical surveys. These boreholes are J5, J7 and J8 (quoted from Abu-ajamieh, 1967) and D-31 (quoted from Davies, 2005). Generally, these boreholes penetrate four rock units. These units from top to bottom are: (1) a thin layer which consists of a mixture of gravel, sand and silt. It represents the topmost part of the lake, (2) a silty clay layer forms the upper main rock unit, (3) a layer represents the water-bearing formation composed of sand and gravel of Quaternary sediments, and (4) the last layer represents the MCM bedrock formation, which is chalky-marl in nature.

The close correlation between the borehole data and the obtained VES models helped to assign various resistivity ranges for the encountered lithologic units (Table 2) and, subsequently, used as a tool for subsurface geoelectrical resistivity interpretation. It is obvious that each lithologic unit is characterized by a wide range of resistivity which indicates that the lithology, salinity and water content play an essential role in relating the different resistivities to a particular lithology.

RESULTS

Litho-resistivity units

The results from the 1-D inversion of the VES stations (Table 1) were compiled and plotted along two profile lines as shown on Figure 2. The two interpreted resistivity vs. depth cross sections are shown in Figures 5 and 6. In these sections the thickness of the subsurface layers and their geological structures are given. Cross section A-A' (Figure 5) represents the behaviour of the northern and eastern sides of the studied area, and is located to the north of the borehole J5. It covers a length of approximately 20 km, extending from sounding station 13 in the west to sounding station 18 in the east. The topographic elevation along this section slopes gently

separation (AB/2) was designed to investigate small scale features and to reveal details of the lithology setting, starting from 1.5 to 350 m.

Owing to the differing character of features in the field apparent resistivity curves, the VES stations show two types of curves. These types were defined in terms of the number of geoelectrical layers and their resistivity relationship. Out of the 20 field curves, 18 field curves at VES stations 1, 2, 3, 4, 5, 6, 7, 8, 9, 10, 11, 13, 14, 15, 16, 17, 18, and 19 reflect the presence of four geoelectric layers where the layers resistivity relationship as $\rho_1 > \rho_2 < \rho_3 > \rho_4$ (e.g., VES station 7, Figure 4a). Two of sounding curves at VES stations 18 and 20 however, reflect the presence of three geoelectric layers

Table 1. Summary of results from computer modelling for all VES stations.

Station no. Figure 2	Elevation (m asl)	No. of layers	Resistivity of layers(ohm-m)				Thickness of layers (m)			RMS error (%)
			ρ_1	ρ_2	ρ_3	ρ_4	t_1	t_2	t_3	
1	852.3	4	385	58	191	19	0.4	1.5	4.45	2.8
2	851.0	4	30	68	128	12	0.9	13	45	3.7
3	851.0	4	11	29	88	18	3.2	12.8	43.6	2.6
4	854.2	4	43	4	93	17	0.31	17.2	27.5	2.9
5	851.8	4	37	5	21	6	0.34	12.8	10.5	1.6
6	851.5	4	11	7	17	4	3.0	9.9	34.3	1.3
7	848.0	4	29	18	38	4	3.0	8.0	35.0	4.2
8	849.2	4	290	66	1218	13	0.8	0.9	8.1	4.7
9	847.5	4	77	33	98	3	1.4	6	37	3.5
10	849.1	4	65	12	130	11	0.8	10.9	12	2.5
11	850.0	4	10	5	180	4	1.7	12.1	41	2.7
12	849.4	4	125	50	180	5	1.0	3.3	25.8	3.1
13	852.5	4	52	24	67	28	0.9	3.8	7.3	0.7
14	849.6	4	93	18	203	38	1.3	1.2	9.5	1.4
15	848.4	4	160	37	273	16	0.8	1.4	19.5	6.6
16	848.0	4	599	62	372	10	0.3	2.0	22.8	3.5
17	847.5	4	298	90	231	9	0.5	2.1	14.5	4.4
18	845.8	3	124	417	32	-	1.3	10.7	-	4.6
19	849.0	4	26	11	40	12	0.8	2.0	16.1	1.2
20	849.2	3	780	1774	10	-	1.5	8.3	-	6.9
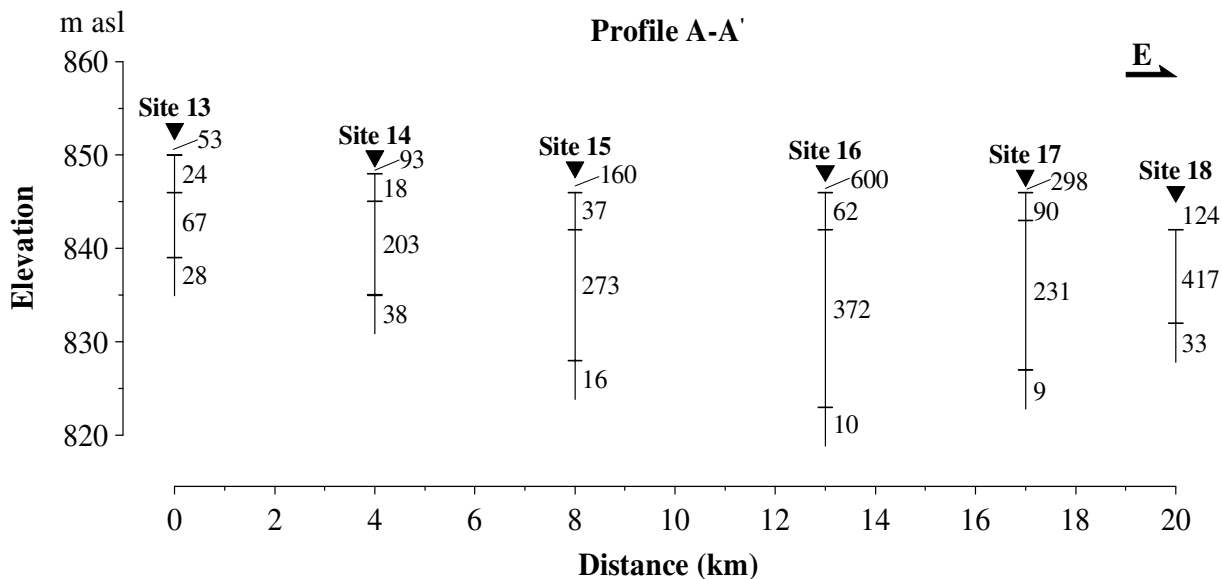
Figure 5. Composite geoelectrical cross section inferred from VES data along A-A' (see Fig. 2 for profile location). Resistivities are in ohm-m.

downward from west to east. The main features of the derived structure, from the surface downward, may be summarized as follows: (1) a thin surface layer of 50 to 600 ohm-m resistivity that is 0.3 to 1.3 m thick. Its resistivity increases, in general, eastwards. The resistivity of this unit is corresponding to a stratum which is mainly composed of wet to dry, fine to coarse sand and gravel in the east margin areas that becomes more silty and fine sand in the western parts, (2) a layer of 20 to 120 ohm-m resistivity and a thickness of about 1 to 4 m, considered

Table 2. Resistivity ranges of various lithologic units.

Borehole Figure 2	Sediment unit	Thickness (m)	Station no.	Resistivity of units (ohm-m)	Thickness of units (m)
J5	Topmost layer	0.8		65	0.8
	Silt and clay	11	10	12	10.9
	Sand and gravel	12		130	12
	MCM formation	-		11	-
J7	Topmost layer	1.7		10	1.7
	Silt and clay	12	11	5	12.05
	Sand and gravel	39.5		180	40
	MCM formation	-		4	-
J8	Topmost layer	0.3		385	0.4
	Silt and clay	1.5	1	58	1.5
	Sand and gravel	4.5		191	4.7
	MCM formation	-		19	-
D-31	Topmost layer	-		77	1.4
	Silt and clay	11	9	33	9.5
	Sand and gravel	-		98	33.5

to have been caused by clayey silt layer at shallower depths and thickening westwards. The high resistivity values of the eastern sites could indicate the dominance of dry coarse sand and gravel which is seen across the borehole J5 (Table 2), (3) the third geoelectric resistivity unit is interpreted as a shallow water-bearing unit sand and gravel that attains resistivity values decreasing generally westwards and varies from 70 to 420 ohm-m. Its thickness increases, in general, from both eastern and western sites towards the central sites and approximately varies from 7 to 23 m, and (4) the lowermost geoelectric resistivity unit, which dominates the study area, is characterized by its relatively low resistivity values ranging from 10 to 40 ohm-m and depth, increasing centralwards, ranging from about 10 to 25 m. This unit is related to the chalky-marl MCM formation of the Belqa Group of bedrock.

Cross section B-B' (Figure 6) represents the behaviour of the southern side of the studied area. The cross section covers a length of approximately 16 km, extending from sounding station 4 in the west to sounding station 8 in the east. The topographic elevation along this section slopes gently downward from both eastern and western sides to the middle parts. A similar structure with four layers is recognized along line B-B' (Figure 2), but with lower resistivity values and some interesting differences. Cross section B-B' (Figure 6) indicate the following layers: (1) a thin surface layer of 11 to 290 ohm-m resistivity that is 0.3 to 3.2 m thick. Its resistivity decreases and its thickness increase from the margin of the playas to the central parts. The resistivity of this unit corresponds to a stratum that is composed mainly of wet to dry, fine to coarse sand and gravel in the margin areas

and becomes more silty and fine sand in the central parts, (2) the second geoelectric resistivity unit shows resistivity values that ranges from 4 to 70 ohm-m and 1 to 13 m thick, and it is considered as a clayey silt layer located at shallower depths and tends to thicken westwards, (3) the third geoelectric resistivity unit is interpreted as a shallow sand and gravel aquifer that attains resistivity values decreasing generally from both eastern and western sides to the central parts and varies from 20 to 1200 ohm-m. The low resistivity values that dominate the central parts may be attributed to either an increase in the salinity of the groundwater, clay members or to the presence of gypsum bands. Borehole D-31 lithology (Davies, 2005) correlates these findings, and (4) a conductive MCM bedrock formation with resistivities of 5 - 20 ohm-m. The depth of this conductor varies along the profile from 27 m to 60 m (Figure 6).

As shown from Figures 5 and 6, the alluvial system within the el-Jufr playa, which overlies the chalky-marl MCM formation bedrock, can be divided into two main stratigraphic sequences having different thicknesses, lithology contents, and geological structures: (1) the upper sediment unit mainly consists of silt and silty clay with sparse of gravels and (2) multiple cycles of gravels and sands characterizing the lower sequence. These are thus discussed.

The upper stratigraphic sequence

The unit in the southern part of the study area is characterized by low resistivity values when compared with the northern and eastern sides that attain relatively high resistivity values. This decrease in resistivity values
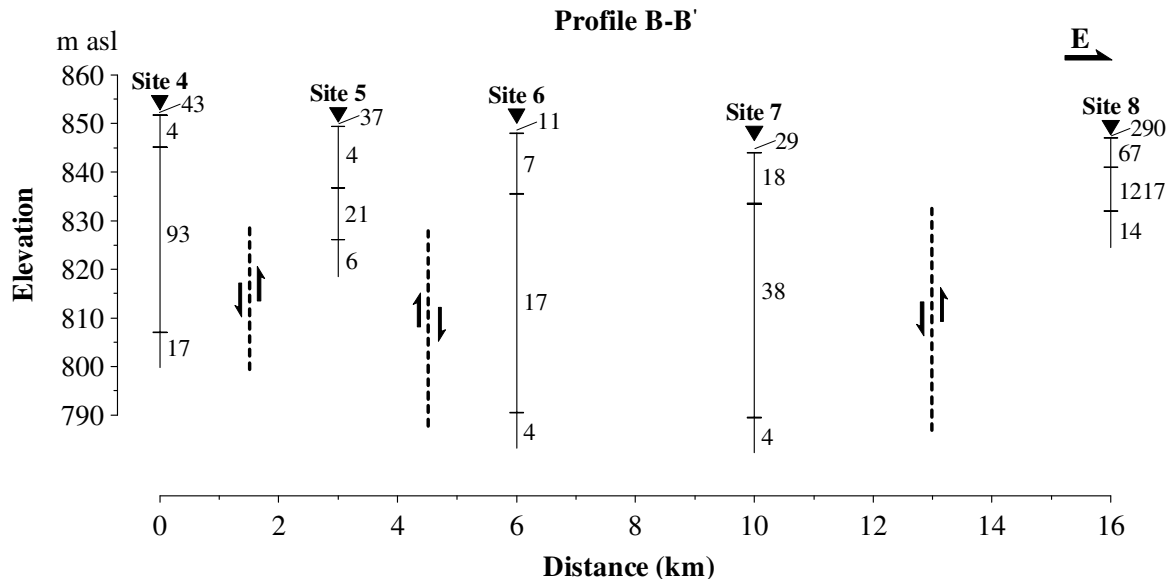
Figure 6. Composite geoelectrical cross section inferred from VES data along B-B' (Figure 2: For profile location). Resistivities are in ohm-m.

from about several ten to hundred ohm meters in the northern and eastern sides (profile A-A', Figure 5) to less than 40 ohm-m in the southern part (profile B-B', Figure 6), can be explained by the existence of more homogeneous and thicker fine silt and clayey sand within the upper unit in the southern part than its northern and eastern parts. In addition, this unit is grading from clay into silt, sand and gravel towards north and east. Average recorded thickness of the upper sediment unit was found to be 2.6 m in the northern and eastern parts and a value of 9.1 m thick was recorded in the southern part (Table 1 and Figures 5 and 6).

The lower stratigraphic sequence

The lower sediment represents the water-bearing unit and mainly consists of gravels and sands grading upward into clayey sand. Along the northern and eastern sides of the study area (profile A-A', Figure 5), the resistivity values of this unit increases eastwards indicating fresh groundwater and/or decreasing clay contents. The thickness of the lower unit along this line gradually increased from both eastern and western sides towards the central parts. Its thickness varies from about 6 m in the margin to about 19 m recorded in the central parts. Relatively, low resistivity values dominate the southern parts (profile B-B', Figure 6) when compared with cross section A-A' (Figure 5), it indicates either an increase of salinity of groundwater in this part or it can be related to a more homogeneous sediment unit of sand and clayey sand. These sediments grade north, west and east into coarse sand with gravels. The recorded thickness of the

lowest stratigraphic unit along profile B-B' (Figure 6) varies from 40 m at site 4 in the west, 10 m at site 5, 50 m at sites 6 and 7 and 8 m thick at site 8 in the eastern side.

Structural elements

As indicated by the geological map of el-Jufr area (Moumani, 2006), the prominent structural element present is the northeast-southwest trending el-Jufr fault which is located in the northeastern part of the study area (Figure 2). The fault is 27 km in length, with a downthrown of about 50 m to the southeast. Based on the interpreted geoelectrical stations (Table 1) and geoelectric cross section (Figure 6), northeast-southwest and north-south trending faults were identified on the basis of the areal distribution and thickness of the interpreted alluvial system. One NE-SW trending fault parallel to el-Jufr fault was located in the central part of the study area. The fault has 20 km length, with a downthrown of about 30 m to the southeast (profile line B-B', Figure 6). Another two faults striking N-S were located in the western and eastern sides. This is in agreement with the results of Moumani (2006) that identify N-S linear feature across the playas floor. Graben and horst structures inside the lake area were formed along the NE-SW and N-S trending faults causing thickening and thinning to the Quaternary sediments. The resulting thickness of the Quaternary sediments derived from the 1-D interpreted geoelectric stations (Table 1) together with the geological structures derived from profile B-B' (Figure 6) were used to construct the isochore map (Figure 7).
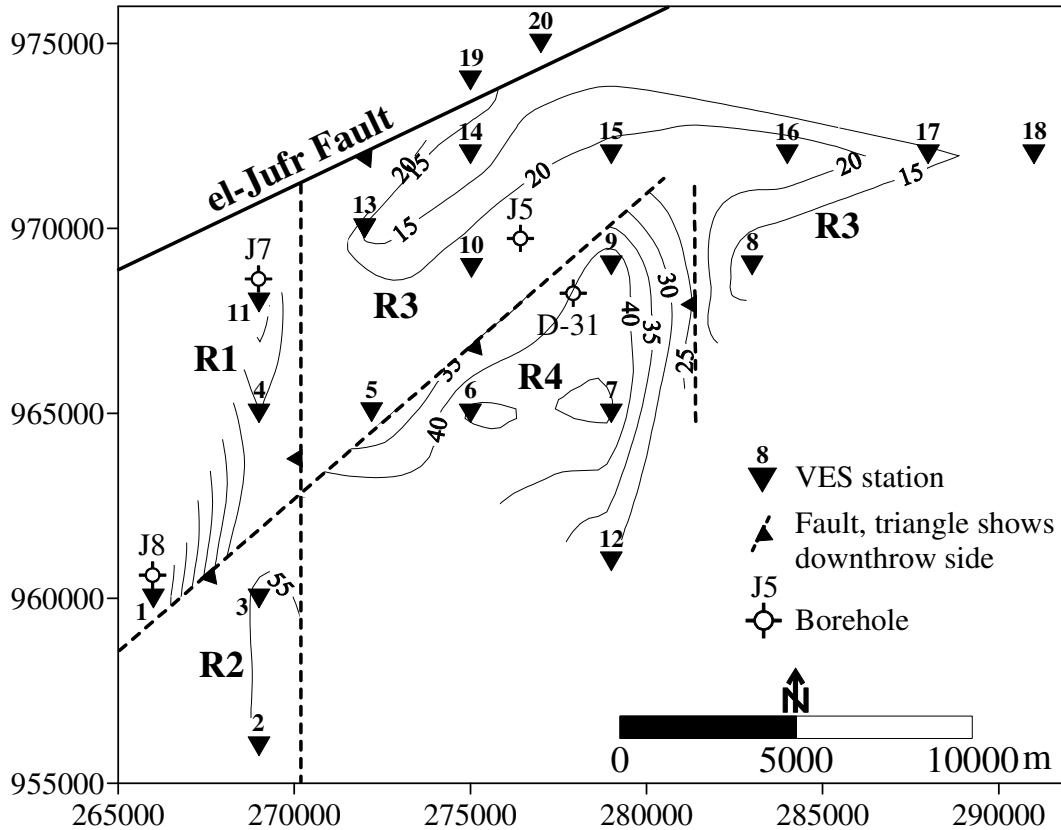
Figure 7. Isopach contour map of the quaternary sediments in relation to inferred structures.

The map indicates the presence of four zones defined in terms of sediment thickness and geological structures which are was marked as R1, R2, R3, and R4 on Figure 7: (1) the first zone, R1, represents a graben structure situated on the northwestern side of the studied area along NE-SW and N-S trending faults. This zone shows Quaternary sediments range in thickness from 6.4 m at site 1 in the southwest margin to 45.1 m at site 4 and about 53.7 m of thickness at site 11 in the extreme north. The increase of thickness towards the northern part could be correlated with the additional aeolian deposits at the western and northwestern margin of the playas, (2) R2 graben along NE-SW and N-S trending faults in the southwestern side shows sediment in the order of 55 m thick at sites 2 and 3, (3) R3, is a horst structure located in the northern and eastern sides along NE-SW and N-S trending faults. The feature attains about 20 m thick of sediment (sites 5 and 10) and thinning eastwards to about 10 m thick (site 18), and (4) R4 is a graben structure located in the south central part along NE-SW and N-S trending faults. It is dominated by about 45 m of Quaternary sediments. It is interesting to note that the thickness of sediment recorded at stations 19 and 20 that were made in the extreme north (Figure 2) varies from 10 to 19 m (Table 1). Where these two stations were located on the upthrow side of el-Jufr Fault (Figure 2).

Conclusions

Twenty vertical electrical sounding (VES) stations were conducted in the el-Jufr playas, southeastern Jordan Plateau, to provide record of Quaternary deposits available in the el-Jufr playa and identify the formations that may have fresh aquifer waters. The results indicate that there are two main stratigraphic units with a thin topmost layer of varied resistivities and thicknesses. The upper unit in the southern part is characterized by low (< 20 ohm-m) resistivity values when compared with relatively high (20 to 100 ohm-m) resistivity values in the northern and eastern sides. This decrease in resistivity values at shallow depths can be explained by more homogeneous fine silty and clayey sand upper sequence in the southern parts. The upper sequence in the northern and eastern parts is characterized by silty sand sediments with sparse of gravels and lack of clays. These sediments are indicative of low-energy alluvial sheet wash and aeolian depositional environments.

The lower unit corresponds to water-bearing unit of gravel and sand, with resistivity values decreasing generally from both eastern and western sides to the central parts. Its thickness increases from both eastern and western sides towards the central side. The low resistivity values that dominate the central parts may

reflect either an increase in the salinity of groundwater, abundant of clays or thick gypsum bands. These sediments reflect periods of higher precipitation and lower evaporation that characterize past trends. This is in good agreement with the results obtained by Davies (2005).

REFERENCES

Abu-ajamieh M (1967). A quantitative assessment of the groundwater potential of the Rijam formation aquifer in the Jafr Basin. Unpublished Report. Natural Resources Authority, Amman, Jordan.

Al-Jayyousi O, Shatanawi M (1995). An analysis of future water policies in Jordan using decision support systems. Int. J. Water Resour. Dev., 11: 315-330.

Batayneh A (2004). Relating geoelectric to hydraulic parameters of the B2/A7 aquifer, central Jordan. Dirasat, 31: 220-233.

Batayneh A (2006). Use of electrical resistivity methods for detecting subsurface fresh and saline water and delineating their interfacial configuration: a case study of the eastern Dead Sea coastal aquifers, Jordan. Hydrogeol. J., 14: 1277-1283.

Batayneh A, Al-Momani I, Jaradat R, Awawdeh M, Rawashdeh A, Ta'any R (2008). Weathering processes effects on the chemistry of the main springs of the Yarmouk Basin, north Jordan. J. Environ. Hydrol., 16: 20.

Batayneh A, Barjous M (2005). Resistivity surveys near a waste-disposal site in Qasr Tuba area of central Jordan. Bull. Eng. Geol. Environ., 64: 287-294.

Batayneh A, Haddadin G, Toubasi U (1999). Using the head-on resistivity method for shallow rock fracture investigations, Ajlun, Jordan. J. Environ. Eng. Geophys., 4: 179-184.

Davies C (2005). Quaternary paleoenvironments and potential for human exploitation of the Jordan Plateau desert interior. Geoarchaeology, 20: 379-400.

Geosoft. Geosoft DAP. http://dap.geosoft.com/geodap/home/default.aspx.

Hadadin N, Tarawneh Z (2007). Environmental issues in Jordan, solutions and recommendations. Am. J. Environ. Sci., 3: 30-36.

Interpex Limited (1999). RESIX-IP User's manual.

Jaber J, Mohsen M (2001). Evaluation of nonconventional water resources supply in Jordan. Desalination 136: 83-92.

Jaffe M, Al-Jayyousi O (2002). Planning models for sustainable water resources development. J. Environ. Plan. Manage., 45: 309-322.

Keller G, Frischknecht F (1966). Electrical methods in Geophysical Prospecting. New York, Pergamon.

Moh'd B (1986). The geology of Wadi Al Buway'ija, Map Sheet No. 3251 IV. Geological Mapping Division, Natural Resources Authority, Jordan, Bull., p. 5.

Mohsen M (2007). Water strategies and potential of desalination in Jordan. Desalination, 203: 27-46.

Mohsen M, Jaber J (2002). Potential of industrial wastewater reuse. Desalination, 152: 281-289.

Moumani K (2006). The geology of Al Jafr area. Map Sheet No. 325-I. Geological Mapping Division, Natural Resources Authority, Jordan, Bull., p. 64.

Orellana E, Mooney H (1966). Master tables and curves for vertical electrical sounding over layered structures. Interciencia, Madrid, p. 34.

Powell J (1989). Stratigraphy and sedimentation of the Phanerozoic rocks in central and south Jordan: Ram and Khreim Groups. Geological Mapping Division, Natural Resources Authority, Jordan, Bull. 11.

Rimawi O, El-Naqa A, Salameh E (1992). Hydrochemical characteristics of groundwater resources in northeastern part of the Valley/Jordan. Dirasat, 19: 87-117.

Ta'any R, Batayneh A, Jaradat R (2007). Evaluation of groundwater quality in the Yarmouk Basin, north Jordan. J. Environ. Hydrol., 15: 28.

Zohdy A (1965). The auxiliary point method of electrical sounding interpretation, and its relationship to the Dar Zarrouk parameters. Geophysics, 30: 644-660.